Eco-evolutionary dynamics of decomposition: scaling up from microbial cooperation to ecosystem function

Elsa Abs[1,2*], Hélène Leman[3,4], and Régis Ferrière[2,5,6]

[1]*Department of Ecology and Evolutionary Biology, University of California, Irvine, CA 92697, USA.*

[2]*Interdisciplinary Center for Interdisciplinary Global Environmental Studies (iGLOBES), CNRS, Ecole Normale Supérieure, Paris Sciences & Lettres University, University of Arizona, Tucson AZ 85721, USA.*

[3]*Numed Inria team, UMPA UMR 5669, Ecole Normale Supérieure, 69364 Lyon, France.*

[4]*Centro de Investigación en Matemáticas, 36240 Guanajuato, México.*

[5]*Department of Ecology and Evolutionary Biology, University of Arizona, Tucson, AZ 85721, USA.*

[6]*Institut de Biologie (IBENS), Ecole Normale Supérieure, Paris Sciences & Lettres University, CNRS, INSERM, 75005 Paris, France.*

Keywords: Degradative exoenzyme, Evolutionary stability, Spatial structure, Scaling limits, Soil carbon stock, Eco-evolutionary feedback, Adaptive dynamics.

Type of Article: Article

Number of words in the abstract: 165

Number of words in the main text: 2883

Number of references: 48

Number of figures: 5

Corresponding author: Elsa Abs. Phone: (520) 208-1112. Email address: eabs@uci.edu

Elsa Abs: eabs@uci.edu: Corresponding author
Hélène Leman: helene.leman@inria.fr
Régis Ferrière: regisf@email.arizona.edu

The decomposition of soil organic matter (SOM) is a critically important process in global terrestrial ecosystems. SOM decomposition is driven by micro-organisms that cooperate by secreting costly extracellular enzymes. This raises a basic puzzle: the stability of microbial decomposition in spite of its evolutionary vulnerability to 'cheaters'—mutant strains that reap the benefits of cooperation while paying a lower cost. Resolving this puzzle requires a multi-scale eco-evolutionary model that captures the spatio-temporal dynamics of molecule-molecule, molecule-cell, and cell-cell interactions. The construction and analysis of such a model shows that the evolutionary stability of decomposition is determined primarily by a combination of soil micro-disturbances, microbial dispersal, and limited soil diffusivity. At the scale of whole-ecosystem function, selection acting on extracellular enzyme production shapes the average soil decomposition rate and carbon stock. As soil diffusivity varies gradually, evolutionary adaptation mediates regime shifts in decomposition. These results suggest that microbial adaptive evolution may be an important factor in the response of soil carbon fluxes to global environmental change.

Microorganisms drive critical ecosystem processes, such as nutrient mineralization and the decomposition of organic matter [Falkowski et al., 2008]. Many of these processes depend on the conversion of complex compounds into smaller products that microbes can assimilate for growth and maintenance. Except in environments where simple nutrients are abundant, microbes rely on extracellular enzymes (exoenzymes) to perform this conversion [Ratledge, 1994]. By doing so, they face a 'public good spatial dilemma' [Allen et al., 2013, Driscoll and Pepper, 2010]. The 'spatial dilemma' over public good production arises because public goods are costly compounds that are secreted outside the cell; reaction products may diffuse away from the enzyme-secreting microbe and therefore benefit not only the individuals producing them, but also neighboring cells [Velicer, 2003, West et al., 2006]. Evolutionary theory predicts that producers of public goods are vulnerable to cheating by individuals that receive the benefits without paying the cost of production. Without some mechanism to support cooperation [Nowak, 2006], public goods production is expected to disappear under exploitation from cheaters. Nonetheless, public goods are ubiquitously produced in all environments, e.g. siderophores that scavenge iron [Buckling et al., 2007, Cordero et al., 2012, Griffin et al., 2004, Julou et al., 2013], polymers that enable biofilm formation [Rainey and Rainey, 2003], and allelopathic compounds that reduce competition [Le Gac and Doebeli, 2010]. Conditions must exist that promote the evolution of exoenzyme production in spite of diffusion.

Evolutionary game theory provides a powerful framework for investigating conditions that favor exoenzyme production [Koch, 1985, Schimel and Weintraub, 2003, Sinsabaugh and Moorhead, 1994]. Evolutionary game-theoretic models have been developed to address competition between exoenzyme-producing and nonproducing (cheating) strains [Allison, 2005, Folse and Allison, 2012, Kaiser et al., 2014, 2015]. Considering the diffusivity of products, these models have highlighted the importance of habitat spatial heterogeneity for the evolution of the production mechanism. For example, organic substrates, microbes, and mineral particles form a three dimensional matrix of aggregates and pore spaces of different sizes in soils [Tisdall and Oades, 1982]. For enzyme-dependent microbes, these physical properties should influence the movement of substrates, enzymes and usable products [Vetter et al., 1998], and the fate of cheating microbes [Allison, 2005, Dobay et al., 2014, Folse and Allison, 2012].

Our understanding of the evolutionary stability of diffusive public goods in general, and of degradative enzyme production in particular, remains incomplete. One limitation of previous models is their focus on two-way competition between two strains, typically a producing strain and a 'pure cheater' or non-producing strain. A key issue here is that mechanisms that promote stability of producers against pure cheaters might fail to prevent 'erosion' of cooperation by mutant strains that produce slightly less of the public good than the wild-type, or resident strain [Ferriere et al., 2002]. Pure cheaters may go locally extinct when they do not receive enough resource produced by cooperators; however, strains that produce less, rather than none, of the public good should be less sensitive to the harm they inflict to the community [Lee et al., 2016]. On the other hand, producers may be vulnerable to pure cheaters and yet resist invasion by strains that invest only slightly less into the common good. We thus expect conditions for the evolutionary stability of

cooperation to be different when considering the recurrent events of mutation of small effects and selection that shape the evolutionary trajectory of exoenzyme production.

To predict the outcome of selection on small-effect variants, we need to evaluate the population growth rate of initially rare mutant types interacting with any given resident type. To achieve this, previous models of microbe-enzyme systems need to be revisited and extended, so that invasion fitness of small-effect mutants can be computed. To describe the interaction of resident strains with mutant cells, which, initially at least, occur in small, spatially localized populations, individual-level modeling of microbe-enzyme systems is required. Previous microbe-enzyme ecological models (reviewed in Abs and Ferrière [2020], Wieder et al. [2015]) are phenomenological, rather than derived by scaling up from microscopic processes acting locally at the level of individual entities. The main difficulty here is to address the extremely different scales that characterize the entities (cells, enzymes, substrates, products) and processes that affect them. Here we derive a hybrid, stochastic-deterministic model that takes this multiplicity of scales into account. By applying the hybrid model to a spatially structured habitat, we elucidate conditions that promote the evolutionary convergence and stability of exoenzyme production. We show that resource diffusivity is a strong control of the selection gradient of exoenzyme production, which determines the average soil decomposition rate and carbon stocks of the whole system. These results suggest that the evolution of microbial exoenzyme production may be an important factor in the response of soil decomposition to environmental change that affect soil properties.

Results

In a single, isolated microsite occupied by a large population, ecosystem dynamics can be approximated by the deterministic '$CDMZ$ model' (equation S.7 in ESM §3.1), and the selection gradient on the exoenzyme allocation trait can easily be derived. At the (non-trivial) ecological equilibrium (c, d, m, z) of a resident population with trait value φ, the growth rate of a mutant strain with trait value φ' is $(1-\varphi')\gamma_M V_{mU}\frac{d}{K_{mU}+d} - d_M$, hence the selection gradient of φ (derivative of the mutant long term growth rate with respect to the mutant trait, evaluated at the resident trait value) equal to $-\gamma_M V_{mU}\frac{d}{K_{mU}+d}$. For any parameter combination and value of the DOC resident equilibrium d, this quantity is always negative: investing in exoenzyme production is always selected against. Thus, any initial level of microbial cooperation will be gradually eroded by the process of mutation-selection, driving the population towards the threshold trait value at which extinction occurs – an instance of evolutionary suicide ([Ferriere, 2000, Ferriere and Legendre, 2013, Parvinen, 2005]). In finite populations, mutant success or failure becomes probabilistic. Due to random genetic drift, cheater phenotypes may fail to invade, and cooperator mutants may occasionally go to fixation. Long term adaptive dynamics driven by rare mutation and selection in finite populations have been studied in a general framework by Champagnat et al. [2007]. They showed that the evolutionary trait dynamics can be described mathematically as a diffusion process whereby a Brownian motion (white noise) is added to a trend driven by the deterministic selection

gradient. To illustrate these general results, Figure 1 shows simulations of a finite microbial population in a single microsite, without and with adaptive evolution of exoenzyme production. In the absence of evolution, simulated populations tend to persist over the total computation time. With evolution, simulated populations generally go extinct within that same time frame. In spite of significant fluctuations due to random genetic drift, adaptive evolution drives the exoenzyme production trait towards the threshold at which the microbial population becomes non-viable.

We address the evolution of exoenzyme production in spatially extended ecosystems using the spatial version of our hybrid stochastic-deterministic model. In a spatially structured soil matrix, exoenzyme producers may resist invasion by non-producer mutants because of the non-uniform distribution of cell types that emerges across microsites, due to local cell dispersal. We ran simulations of the spatial model to test the consequences of this mechanism for the evolution of exoenzyme production as a continuous trait, as opposed to an all-or-nothing character (as in previous studies). To circumvent the issue of prohibitive computation time, we parallelized the simulations of an ensemble of pairwise contests between slightly different strains, one taken as 'resident' (initially at stationary state) and the other as 'mutant (initially rare, see Fig. 2 and Supplementary Material § 3.4). Spatial segregation of resident and mutant strains across microsites is key to the evolutionary stability of exoenzyme production. In the absence of micro-disturbances that empty sites out, different strains will be mixed by dispersal. When that is the case, a slightly cheating mutant strain always invades and spreads across the lattice. This is because the diffusion of DOC creates local conditions (within microsites) that are even more unfavorable to the resident strain than in the case of a single, isolated microsite. The long-term consequence is evolutionary suicide, as in the case of a well-mixed population. When micro-disturbances are taken into account, the dispersal process will – provided it is fast enough – drive the spatial segregation of resident and mutant strains among microsites. The local resource pool (DOC) to which cells of a given strain have access is determined by their own exoenzyme production, and the diffusion of DOC from nearby microsites. The local growth of a strain then determines its chance of colonizing nearby empty microsites and spreading across the lattice. Depending on the DOC diffusion rate, spatial segregation of strains at micro-scale can promote resistance of exoenzyme producing strains against invasion by cheater strains that produce slightly less exoenzyme (negative selection against cheating); and favor invasion of exoenzyme producing strains by strains that produce exoenzyme at larger rates (positive selection for cooperation). Figure 2 shows an example of the latter. To further evaluate the effect of diffusion on the selection gradient of exoenzyme production, we measured the invasion fitness of mutant strains in pairwise competition with slightly different resident strains, across a range of soil diffusion rates, σ_{diff}. Based on the formal analysis of adaptive evolutionary dynamics in finite populations [Champagnat et al., 2007], a proxy for invasion fitness is given by the product of the mutant probability of survival with the long-term population growth rate of surviving mutant populations. The rationale is that deleterious mutants may experience positive growth due to genetic drift, but their overal probability of survival is low; in contrast, advantageous mutants that differ only slightly from the resident strain tend to grow slowly, but their survival

probability is high. In Figure 3, pairwise competition simulations run across the trait range $0.05 - 0.25$, under different values of the soil diffusion rate, show a clear pattern of directional selection for increasing exoenzyme production when soil diffusion is low (cooperator mutants have positive fitness), and directional selection for decreasing φ towards zero when soil diffusion is high (cheater mutants have positive fitness). For intermerdiate soil diffusion rates, there is stabilizing selection around an intermediate value of φ (evolutionarily stable strategy, or ESS), which tends to increase as soil diffusion decreases. Thus, for intermediate diffusion, the spatial model predicts (i) existence of an exoenzyme production ESS that resists invasion by cheating strains, and (ii) evolutionary convergence to the ESS from ancestral strains with minimal exoenzyme production.

In nature, parameters such as the diffusion rate are expected to depend on environmental features such as soil properties and precipitation, that can vary widely across ecosystems. We find that resource diffusion has a major influence on the selection gradient of exoenzyme production (Fig. 3). To further characterize this influence and investigate its ecosystem-level, functional consequences, we extracted the pattern of variation of the exoenzyme production ESS along a gradient of diffusion rates (Fig. 4a) and computed the corresponding decomposition rate (Fig. 4b) and soil C stock (Fig. 4c) at lattice scale. The diffusion gradient could represent spatial variation across ecosystems, or a temporal sequence driven by some external environmental factor, e.g. a gradual change in precipitation. Figure 4a shows that decreasing diffusion from 10^{-5} to 10^{-7} drives a significant evolutionary change in exoenzyme production, from 0.05 to 0.25. The evolutionary response of exoenzyme production to varying diffusion feeds back to the ecological state of the whole lattice and alters ecosystem-level function: the average, lattice-scale decomposition rate rises three-fold as exoenzyme production adapts to reduced diffusion (Fig. 4b), driving an 80% drop in the soil C stock (Fig. 4c). Note that the patterns in Figures 4b and 4c closely match the response of the exoenzyme allocation ESS to varying diffusion (Fig. 4a), and that the error bars reflecting differences in the average values among simulations are very small compared to the differences induced by the change in φ. This shows that the process of evolutionary microbial adaptation can induce much stronger variation in the lattice-scale ecosystem properties (decomposition rate, soil C stock) than stochasticity.

Discussion

Soil microbial decomposition involves the production of exoenzymes and uptake of the products of enzyme-driven depolymerization of dead organic matter. These products form a diffusive public good, which is vulnerable to exploitation by cheaters. To elucidate conditions under which decomposition, as an outcome of microbial cooperation, is evolutionarily stable against mutations of small effects, we constructed a spatial model of soil microbe-enzyme decomposition which accounts for the finite size of microbial populations at the microscopic scale of microbial interactions.

Deterministic models of microbe-enzyme driven decomposition were first introduced by Schimel and Weintraub [2003] for 'well-mixed' systems. Our work shows in a rigorous mathematical

framework that Schimel and Weintraub [2003]'s model and subsequent variants (reviewed in Abs and Ferrière [2020]) are consistent with microscopic processes acting at the level of individual entities (cells, molecules). Starting from a five-compartment model including SOC and DOC molecules, microbial cells, enzyme molecules, and enzyme-SOC molecular complexes, we found that the population size of cells and molecules and some of the stochastic process rates could be rescaled to yield Schimel and Weintraub [2003] four-compartment deterministic $CDMZ$ model. As a side note, we could not find further or alternate rescaling to reduce the dimension of the system to three compartments (CDM or CMZ or DMZ). One can also prove that in all two-compartment models the equilibrium with positive cell population size is always unstable, which means that the cell population either goes extinct or grows unboundedly. Thus, the four-compartment $CDMZ$ structure seems to be the simplest that is consistent with the individual-level processes under consideration.

The deterministic $CDMZ$ model, however, cannot be used to capture the dynamics of a spatially explicit system in which a finite number of cells and molecules interact within their local neighborhood. From the stochastic $CDMZ$ model we obtained a hybrid stochastic-deterministic model for local populations and interactions by assuming that the size of the molecular populations (C, D, Z) is typically much larger than the size of the cellular population (M). A spatially explicit model can then be assembled by coupling hybrid models to form a lattice of microsites. Microsite and lattice-level parameters can be specified to capture the millimeter and centimeter scale, respectively, which distinguishes this model from previous individual-based simulation models of decomposition [Allison, 2005, Folse and Allison, 2012, Kaiser et al., 2014, 2015]. In particular, the model can accommodate changes in the strength of competition within a colony (individuals of the same strain) by modifying the size of microsites, and between colonies of different strains by modifying the size of the lattice. By modeling the dynamics of cell populations and decomposition within and between microsites, we can take an evolutionary stance and address the effect of spatially heterogeneous population size and growth on the dynamics of invasion of a mutant genotype in the established population of the wild-type (resident) strain.

It has long been known that environmental spatial structure can promote cooperation by facilitating benefit-sharing among cooperators. This was shown originally for pairwise interactions and later in the case of diffusive public goods. However, early models of diffusive public goods [Driscoll and Pepper, 2010, Ross-Gillespie et al., 2007, West and Buckling, 2003] represented space only implicitly and were therefore limited in their ability to identify conditions for the evolutionary stability of cooperation. Allison [2005] spatially explicit, individual-based simulation model of enzymatic litter decomposition backed up the expectation that the rate of products diffusion was key to the stability of cooperation. This and subsequent related models [Allison, 2012, Dobay et al., 2014, Folse and Allison, 2012, Kaiser et al., 2014, 2015], however, focused on competition between two or a small set of exoenzyme production genotypes, e.g. a producing strain and a non-producing ('pure cheater') strain. Our analysis goes further by predicting the evolutionary dynamics of exoenzyme production as a quantitative trait, varying continuously due to random mutation of

small effect.

Just like soil diffusion was identified as a critical factor for the stability of a producing strain against invasion by pure cheaters [Allison, 2005, Dobay et al., 2014], our model shows that the diffusion rate determines the evolutionarily stable investment in exoenzyme production. We did not observe evolutionary branching and coexistence in our simulations, but they might occur in regions of the parameter space that we have not yet explored. Otherwise, instances of coexistence reported by Allison [2005] and Kaiser et al. [2014, 2015] would likely be evolutionarily unstable and/or inaccessible to evolution by mutation of small effects.

Finally, our model shows how variation in evolutionarily stable exoenzyme production feeds back to ecosystem macroscopic properties such as the decomposition rate and soil C stock at lattice scale. The model predicts that if environmental change, such as variation in soil physical properties or precipitation, drives changes in soil diffusion, then the microbial community may respond evolutionarily, and in return, the microorganisms' evolutionary, adaptive response may substantially impact ecosystem function. Previous models investigated how soil functional properties such as decomposition, heterotrophic respiration, and carbon stock, respond to variation in soil moisture due to variable precipitation [Homyak et al., 2018, Zhang et al., 2014]. Focusing on experimental data from semi-arid savannah-type ecosystem subject to contrasted precipitation regimes, Zhang et al. [2014] used model-data assimilation to demonstrate the importance of water saturation as a control of enzyme activity and DOC uptake, and of the accumulation and storage of enzymes and DOC (that is temporarily inaccessible to microbes) in the dry soil pores during dry periods. Our results show that microbial evolution of exoenzyme production, in and of itself, can drive strong ecosystem responses to the effect of soil moisture variation on soil diffusion. Droughts that affect soil diffusion may also elicit microbial physiological responses ([Allison and Goulden, 2017]) such as higher investment in osmolyte production, potentially at the expense of exoenzyme production ([Malik et al., 2019]); extensions of our model could evaluate the consequences for soil carbon loss. Additionally, one could explore the relative effect on decomposition and heterotrophic respiration of microbial physiological ([Homyak et al., 2018, Zhang et al., 2014]) and evolutionary responses to the spatial heterogeneity of soil water distribution. Using Melbourne and Chesson [2006]'s theory of scale transition, recent work by Chakrawal et al. [2019] establishes a powerful framework to incorporate soil heterogeneity in models of decomposition.

We conclude that large ecosystem effects may result from the evolutionary adaptive response of microbial populations to changes in soil abiotic properties like diffusion. This calls for a more general investigation of the large-scale ecosystem consequences of soil microbial evolution in response to global environmental change, such as climate warming. The thermal dependence of microbe-enzyme biochemical processes involved in decomposition can radically change the global projections of soil C in response to climate warming [Wieder et al., 2013]. Future research is warranted to evaluate how microbial evolutionary adaptation to warming may further alter global projections of terrestrial carbon cycling.

Methods

To construct a spatially explicit model of microbe-enzyme decomposition, we focus on bacterial cells and unprotected soil organic carbon [Davidson and Janssens, 2006] and we assume nitrogen and phosphorus to be non limiting. Space is modelled as a two-dimensional lattice of microsites, with each microsite potentially occupied by a cell colony. Decomposition is seen as a microbial public good game, whereby individual microorganisms invest resources into the production of degradative exoenzymes. Exoenzyme molecules bind soil organic carbon (SOC) molecules and catalyse the depolymerization of SOC into dissolved organic carbon (DOC) molecules. DOC molecules occurring in a microsite may be uptaken and metabolized by cells present in the microsite, resulting in cell growth and exoenzyme production. The fraction of uptaken DOC that is invested by a cell in exoenzyme production, as opposed to cell biomass production, is denoted by φ. This is the focal trait that characterizes the microbial phenotype, for which we assume heritable variation, originating in mutation [Alster et al., 2016, Trivedi et al., 2016].

Ecosystem dynamics at microsite scale. We assume that cells, enzymes, substrates (SOC) and products (DOC) are well-mixed within each microsite. We assume that only dissolved products (DOC) can diffuse and offspring cells can disperse between neighboring microsites. Additional processes operating at the level of individual entities are: cell respiration, parametrized by the energetic cost of cell tissue and the energetic cost of enzyme molecules; cell death and enzyme degradation, at constant rates; cell division, determined by accrued and stored resources reaching a threshold within the cell; formation and reaction or dissociation of SOC-enzyme complexes. Additional processes operating at the level of microsites are: external inputs of SOC and DOC, losses of SOC and DOC (leaching), diffusion of DOC, random disturbances causing cell colony death and microsite 'opening' to cell dispersal. We measure the abundance of all entities in units of carbon mass. The 'local' dynamics of decomposition within a microsite involves fluxes in and out of five local compartments: microbial cells (biomass M), enzymes (Z), SOC (C), SOC-enzyme complexes (X), and DOC (D) (Fig. 5a). To scale up the dynamics of decomposition from microscopic, stochastic processes, we take the following steps:

1. We define the stochastic processes acting at the level of C, D, M, Z, X entities (molecules, cells) (Fig. 5a).

2. We apply appropriate rescaling on the rates of complex (X) formation, reaction or dissociation, to express that complex dissociation and complex decomposition are much faster than complex formation. By doing so, we reduce the stochastic model to four state variables (C, D, M, Z) (Fig. 5b).

3. We rescale the reduced stochastic model into a hybrid, stochastic-deterministic model, in which only M is treated as a integer-valued variable. This is achieved by considering that a cell is of the order of 10^7 times larger than one enzyme or substrate (SOC) molecule, and 10^{10} times larger than one product (DOC) molecule. Within a given volume, the number of cells is

between 10^{-5} to 10^{-10} times smaller than the number of molecules of enzyme, SOC or DOC. As a consequence, the dynamics of cells and the dynamics of enzyme, SOC and DOC do not unfold on the same scales. The events affecting Z, C and D are much faster and more numerous than events affecting M. As a consequence, we can treat the dynamics of Z, C and D as deterministic over time bouts of constant cell population. Mathematically, the resulting hybrid, stochastic-deterministic model is a Piecewise Deterministic Markovian Process, or PDMP.

4. Finally, we further simplify the hybrid model by noting that the growth of individual cells is driven by events (resource uptake) that occur on the same timescale as the events affecting Z, C, and D in the stochastic $CDMZ$ model defined at Step 2. Then the consumption of D by cells is no longer a stochastic process but instead depends deterministically on M. Cell production thus becomes nearly deterministic, and the only remaining stochastic process is cell death. Even though the rigorous proof of step 4 is beyond the scope of the paper, we will adopt this approximation as we develop the spatially explicit extension of the model.

We refer to the electronic supplementary material (ESM) §1, for mathematical derivations involved in each step. In ESM §1.1 and Tables S1 and S2 we rigorously define the five-variable stochastic process (Step 1). In ESM §1.1 and Table S2, we prove the reduction to the four-variable $CDMZ$ stochastic model (Step 2). In ESM §1.2, we construct and thereby prove the existence of the PDMP model.

According to the PDMP model, the ecosystem dynamics are driven by jumps of the finite cell number M (corresponding to cell birth and death events), interspersed with periods of continuous change in the abundance of enzyme, SOC, and DOC. Cell deaths occur at random times, at rate d_M. When a cell dies, it is removed from the system and its carbon content is recycled into SOC and DOC. Birth events occur deterministically once the cell has experienced enough resource uptake events to assimilate and store the amount of DOC corresponding to one cell. Step 4 allows us to model the amount S_i of DOC stored within cell i as governed by

$$\frac{dS_i(t)}{dt} = \alpha(1-\varphi)\gamma_M V_{mU}\frac{d}{K_{mU}+d},$$

where d measures the rescaled, continuously-varying amount of DOC, in carbon mass unit, and α is the structural cost of one cell in unit of number of DOC molecules. Thus, α sets the threshold on S_i at which the cell divides and both mother and daugther cells' reserve is set back to 0. The other parameters are φ, the fraction of investment in exoenzyme production vs. cell growth; γ_M, the microbial carbon mass production fraction, or microbial growth efficiency (MGE); V_{mU} and K_{mU}, the maximum uptake rate and uptake half-saturation constant, respectively, of the Michaelis-Menten uptake function.

For a given number of cells, M, the change in enzyme, SOC and DOC are governed by

$$\begin{cases} z'(t) = \varphi\alpha\omega_D V_{mU}\gamma_Z \dfrac{d}{K_{mU}+d} M - d_Z z \\ c'(t) = I_C - l_C c - V_{mD} z c \\ d'(t) = I_D - l_D d + V_{mD} z c + (1-l) d_Z z - \varphi\alpha V_{mU} \dfrac{d}{K_{mU}+d} M, \end{cases}$$

where z and c measure the rescaled, continuously-varying amount of enzymes and SOC in carbon mass unit; ω_D is the carbon mass of a DOC molecule, γ_Z is the enzyme carbon mass production fraction, d_Z is the enzyme carbon mass deactivation rate, I_C and I_D are the external inputs of C and D respectively, l_C and l_D are the leaching rates of C and D, V_{mD} is the maximum decomposition rate when C is not limiting, and l is the fraction of deactivated z that is leached instead of recycled. Finally, the capacity of the system is fixed by a parameter K, which calibrates the number of interacting cells at any time in one microsite, empirically estimated to be of the order of 10 to 100 [Raynaud and Nunan, 2014]. See ESM §1.2 for more detail about model rescaling and ESM §1.1 for further discussion of parameter K. With very large K, the model hybrid stochastic-deterministic model can be approximated by a fully deterministic model which takes the form of a system of four ordinary differential equations, similar to the $CDMZ$ microbial decomposition model first introduced by Allison et al. [2010].

Spatial extension of ecosystem dynamics to lattice scale. In order to model the process of mutant invasion in a resident population of cells, we extend the simplified PDMP model to a spatially explicit, spatially homogeneous lattice of microsites. Spatial homogeneity means that all sites have the same capacity, K, and the same abiotic parameters, I_C, I_D, l_C, l_D and l. To this end, we couple PDMP models locally among microsites, by accounting for the diffusion of products (DOC) and dispersal of cells between adjacent microsites. The DOC diffusion between microsites is modelled by approximating a continuous diffusion with a Euler scheme in which time is discretized with a fixed time step interval, τ_{diff}. At each time, a step of the Euler scheme associated with the diffusion equation

$$\frac{d}{dt} d(x,t) = \sigma_{\text{diff}} \Delta d(x,t)$$

is realized for the variable d, where x is the spatial position and σ_{diff} is the DOC diffusion coefficient. Space discretization in the Euler scheme is chosen to match the habitat lattice structure. Cell dispersal may occur following birth events. The daughter cell is added to the mother cell colony with probability $1 - p_{disp}$, or the cell disperses (with probability p_{disp}) to one of the four neighbouring microsites. If empty microsites (one at least) are available in the neighborhood, the dispersing cell moves to one of them, drawn randomly. If all neighboring microsites are occupied, there is a probability p_{open} that a micro-disturbance of the soil strikes and opens one of them, which then becomes occupied by the dispersing cell, while c and d released by the dead cells are recycled locally. If no microsite opens (with probability $1 - p_{open}$), the dispersal event is unsuccessful and the daughter cell remains in its maternal microsite. The dynamics of each microsite is recalculated

between two diffusion steps and after each cell birth or death event. See ESM §2 for further detail.

Mutant invasion and selection. Adaptive evolution of the exoenzyme allocation fraction trait, φ, is modelled by considering trait mutation that cause the trait of daughter cells to differ from the maternal trait value. There is a constant probability of mutation at each birth event, and the value of a mutated trait is assumed to be normally distributed around the maternal value, with small variance to represent mutations of small effect. Cells that have the same φ value belong to the same "strain". Any new mutant strain arises in a system where the abundance of SOC, DOC and exoenzymes has been controlled by the already established, 'resident' strains. Selection occurs because strains with different φ will differentially succeed at acquiring the DOC resource for which they compete. The direction and strength of selection on the evolving trait is measured by the selection gradient of the trait, which can be derived from the probability of invasion of an initially rare mutant strain arising in the population stationary state of a resident strain ([Ferriere and Gatto, 1995, Metz et al., 1992], see Champagnat et al. [2007] for the extension to finite populations). Relative to a given strain, we call "cheaters" mutants that invest less in exoenzyme production (smaller φ) and "cooperators" mutants that invest more in exoenzyme production (larger φ).

Data availability

The simulations and figures that support the findings of this study were coded with C++ and R. The code files have been deposited in "IBMAbsLemFer" (https://github.com/elsaabs/IBMAbsLemFer).

References

Elsa Abs and Régis Ferrière. Modeling microbial dynamics and soil respiration, effect of climate change. in biogeochemical cycles: Ecological drivers and environmental impact. American Geophysical Union, 2020.

Benjamin Allen, Jeff Gore, and Martin A Nowak. Spatial dilemmas of diffusible public goods. Elife, 2:e01169, 2013.

SD Allison. A trait-based approach for modelling microbial litter decomposition. Ecology letters, 15(9):1058–1070, 2012.

Steven D Allison. Cheaters, diffusion and nutrients constrain decomposition by microbial enzymes in spatially structured environments. Ecology Letters, 8(6):626–635, 2005.

Steven D Allison and Michael L Goulden. Consequences of drought tolerance traits for microbial decomposition in the dement model. Soil Biology and Biochemistry, 107:104–113, 2017.

Steven D Allison, Matthew D Wallenstein, and Mark A Bradford. Soil-carbon response to warming dependent on microbial physiology. Nature Geoscience, 3(5):336, 2010.

Charlotte J Alster, Peter Baas, Matthew D Wallenstein, Nels G Johnson, and Joseph C von Fischer. Temperature sensitivity as a microbial trait using parameters from macromolecular rate theory. Frontiers in microbiology, 7:1821, 2016.

Angus Buckling, Freya Harrison, Michiel Vos, Michael A Brockhurst, Andy Gardner, Stuart A West, and Ashleigh Griffin. Siderophore-mediated cooperation and virulence in pseudomonas aeruginosa. FEMS microbiology ecology, 62(2):135–141, 2007.

Arjun Chakrawal, Anke M Herrmann, et al. Dynamic upscaling of decomposition kinetics for carbon cycling models. submitted, 2019.

Nicolas Champagnat, Amaury Lambert, et al. Evolution of discrete populations and the canonical diffusion of adaptive dynamics. The Annals of Applied Probability, 17(1):102–155, 2007.

Otto X Cordero, Laure-Anne Ventouras, Edward F DeLong, and Martin F Polz. Public good dynamics drive evolution of iron acquisition strategies in natural bacterioplankton populations. Proceedings of the National Academy of Sciences, 109(49):20059–20064, 2012.

Eric A Davidson and Ivan A Janssens. Temperature sensitivity of soil carbon decomposition and feedbacks to climate change. Nature, 440(7081):165, 2006.

A Dobay, HC Bagheri, A Messina, R Kümmerli, and DJ Rankin. Interaction effects of cell diffusion, cell density and public goods properties on the evolution of cooperation in digital microbes. Journal of evolutionary biology, 27(9):1869–1877, 2014.

William W Driscoll and John W Pepper. Theory for the evolution of diffusible external goods. Evolution: International Journal of Organic Evolution, 64(9):2682–2687, 2010.

PG Falkowski, T Fenchel, and EF Delong. The microbial engines that drive earth'92s biogeochemical cycles. Science, 320:1034–1039, 2008.

R Ferriere. Spatial structure and viability of small populations. Revue d'Ecologie-La Terre et la Vie, pages 135–138, 2000.

R Ferriere and Marino Gatto. Lyapunov exponents and the mathematics of invasion in oscillatory or chaotic populations. Theoretical Population Biology, 48(2):126–171, 1995.

Regis Ferriere and Stéphane Legendre. Eco-evolutionary feedbacks, adaptive dynamics and evolutionary rescue theory. Philosophical Transactions of the Royal Society B: Biological Sciences, 368(1610):20120081, 2013.

Régis Ferriere, Judith L Bronstein, Sergio Rinaldi, Richard Law, and Mathias Gauduchon. Cheating and the evolutionary stability of mutualisms. Proceedings of the Royal Society of London. Series B: Biological Sciences, 269(1493):773–780, 2002.

Henry Joseph Folse and Steven D Allison. Cooperation, competition, and coalitions in enzyme-producing microbes: social evolution and nutrient depolymerization rates. Frontiers in microbiology, 3:338, 2012.

Ashleigh S Griffin, Stuart A West, and Angus Buckling. Cooperation and competition in pathogenic bacteria. Nature, 430(7003):1024, 2004.

Peter M Homyak, Joseph C Blankinship, Eric W Slessarev, Sean M Schaeffer, Stefano Manzoni, and Joshua P Schimel. Effects of altered dry season length and plant inputs on soluble soil carbon. Ecology, 99(10):2348–2362, 2018.

Thomas Julou, Thierry Mora, Laurent Guillon, Vincent Croquette, Isabelle J Schalk, David Bensimon, and Nicolas Desprat. Cell–cell contacts confine public goods diffusion inside pseudomonas aeruginosa clonal microcolonies. Proceedings of the National Academy of Sciences, 110(31):12577–12582, 2013.

Christina Kaiser, Oskar Franklin, Ulf Dieckmann, and Andreas Richter. Microbial community dynamics alleviate stoichiometric constraints during litter decay. Ecology letters, 17(6):680–690, 2014.

Christina Kaiser, Oskar Franklin, Andreas Richter, and Ulf Dieckmann. Social dynamics within decomposer communities lead to nitrogen retention and organic matter build-up in soils. Nature communications, 6:8960, 2015.

Arthur L Koch. The macroeconomics of bacterial growth. Special Publications of the Society for General Microbiology[SPEC. PUBL. SOC. GEN. MICROBIOL.]. 1985., 1985.

Mickael Le Gac and Michael Doebeli. Environmental viscosity does not affect the evolution of cooperation during experimental evolution of colicigenic bacteria. Evolution: International Journal of Organic Evolution, 64(2):522–533, 2010.

William Lee, Minus van Baalen, and Vincent AA Jansen. Siderophore production and the evolution of investment in a public good: an adaptive dynamics approach to kin selection. Journal of theoretical biology, 388:61–71, 2016.

Ashish A Malik, Jennifer BH Martiny, Eoin L Brodie, Adam C Martiny, Kathleen K Treseder, and Steven D Allison. Defining trait-based microbial strategies with consequences for soil carbon cycling under climate change. The ISME journal, pages 1–9, 2019.

Brett A Melbourne and Peter Chesson. The scale transition: scaling up population dynamics with field data. Ecology, 87(6):1478–1488, 2006.

Johan AJ Metz, Roger M Nisbet, and Stefan AH Geritz. How should we define ?fitness? for general ecological scenarios? Trends in Ecology & Evolution, 7(6):198–202, 1992.

Martin A Nowak. Five rules for the evolution of cooperation. science, 314(5805):1560–1563, 2006.

Kalle Parvinen. Evolutionary suicide. Acta biotheoretica, 53(3):241–264, 2005.

Paul B Rainey and Katrina Rainey. Evolution of cooperation and conflict in experimental bacterial populations. Nature, 425(6953):72, 2003.

Colin Ratledge. Biodegradation of oils, fats and fatty acids. pages 89–141, 1994.

Xavier Raynaud and Naoise Nunan. Spatial ecology of bacteria at the microscale in soil. PLoS One, 9(1):e87217, 2014.

Adin Ross-Gillespie, Andy Gardner, Stuart A West, and Ashleigh S Griffin. Frequency dependence and cooperation: theory and a test with bacteria. The American Naturalist, 170(3):331–342, 2007.

Joshua P Schimel and Michael N Weintraub. The implications of exoenzyme activity on microbial carbon and nitrogen limitation in soil: a theoretical model. Soil Biology and Biochemistry, 35(4): 549–563, 2003.

RL Sinsabaugh and DL Moorhead. Resource allocation to extracellular enzyme production: a model for nitrogen and phosphorus control of litter decomposition. Soil biology and biochemistry, 26(10):1305–1311, 1994.

Judith M Tisdall and J_M Oades. Organic matter and water-stable aggregates in soils. Journal of soil science, 33(2):141–163, 1982.

Pankaj Trivedi, Manuel Delgado-Baquerizo, Chanda Trivedi, Hangwei Hu, Ian C Anderson, Thomas C Jeffries, Jizhong Zhou, and Brajesh K Singh. Microbial regulation of the soil carbon cycle: evidence from gene–enzyme relationships. The ISME journal, 10(11):2593, 2016.

Gregory J Velicer. Social strife in the microbial world. Trends in microbiology, 11(7):330–337, 2003.

YA Vetter, JW Deming, PA Jumars, and BB Krieger-Brockett. A predictive model of bacterial foraging by means of freely released extracellular enzymes. Microbial ecology, 36(1):75–92, 1998.

Stuart A West and Angus Buckling. Cooperation, virulence and siderophore production in bacterial parasites. Proceedings of the Royal Society of London B: Biological Sciences, 270(1510):37–44, 2003.

Stuart A West, Ashleigh S Griffin, Andy Gardner, and Stephen P Diggle. Social evolution theory for microorganisms. Nature reviews microbiology, 4(8):597, 2006.

William R Wieder, Gordon B Bonan, and Steven D Allison. Global soil carbon projections are improved by modelling microbial processes. Nature Climate Change, 3(10):909, 2013.

William R Wieder, Steven D Allison, Eric A Davidson, Katerina Georgiou, Oleksandra Hararuk, Yujie He, Francesca Hopkins, Yiqi Luo, Matthew J Smith, Benjamin Sulman, et al. Explicitly representing soil microbial processes in earth system models. Global Biogeochemical Cycles, 29 (10):1782–1800, 2015.

Xia Zhang, Guo-Yue Niu, Ahmed S Elshall, Ming Ye, Greg A Barron-Gafford, and Mitch Pavao-Zuckerman. Assessing five evolving microbial enzyme models against field measurements from a semiarid savannah—what are the mechanisms of soil respiration pulses? Geophysical Research Letters, 41(18):6428–6434, 2014.

Acknowledgements

We thank Steven Allison, Rachel Gallery, Pierre-Henri Gouyon, Moira Hough, Laura Meredith, Mitch Pavao-Zuckerman and Scott Saleska for discussion. E.A. was supported by fellowships from Ecole Doctorale Frontières du Vivant and MemoLife Laboratory of Excellence (PIA-10-LBX-54). H.L. acknowledges support from CONACyT-MEXICO, CONACYT grant CB2015-01/250590, the foundation Sofía Kovalevskaia of SMM and the Chair "Modélisation Mathématique et Biodiversité" of VEOLIA-Ecole Polytechnique-MNHN-F.X. R.F. acknowledges support from FACE Partner University Fund, CNRS Mission pour les Initiatives Transverses et Interdisciplinaires (MITI), PSL University (IRIS OCAV and PSL-University of Arizona Mobility Program), and a grant from the Dimensions of Biodiversity program of the United States National Science Foundation (DEB-1831493).

Author contributions

E.A., H.L. and R.F. conceived the research and developed the model. H.L. conducted mathematical analysis. E.A. and H.L. wrote code and performed simulations. E.A., H.L. and R.F. contributed to writing the manuscript.

Competing interests

We declare we have no competing interests.

Additional information

Supplementary material is available for this paper at https://doi.org/xxx.

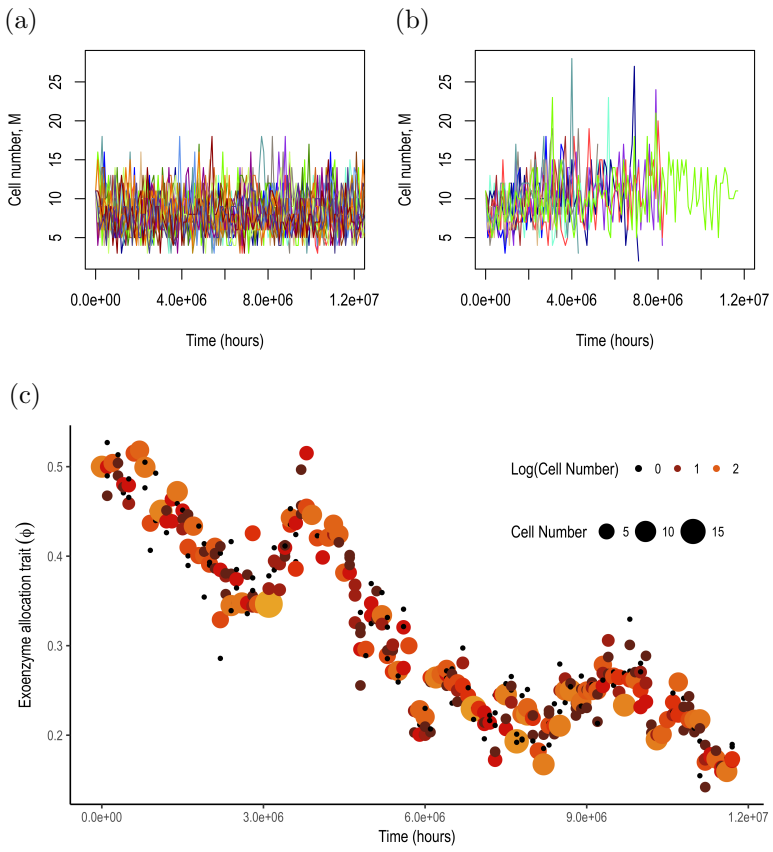

Figure 1. Dynamics of the cell population size and microbial trait φ, with and without mutation. The ancestral cell trait value is $\varphi = 0.5$. (a) Cell population dynamics without mutation. Due to demographic stochasticity, the populations fluctuate around the deterministically predicted steady state of 10 individuals. (b) Cell population dynamics with mutation, with probability $p_{mut} = 0.1$. Ten simulation runs are shown. As populations evolve, they reach the minimum viable value of the enzyme production trait, φ, and go extinct in most of the 10 runs. (c) Evolution of enzyme allocation fraction, φ in one of the simulations from (b). In (a) and (b), 10 simulation runs are shown. All simulations were initialized with a monomorphic M population with trait $\varphi = 0.5$. In all simulations, the four variables c, d, z, M were initialized at the steady state values predicted by the deterministic model with $\varphi = 0.5$. All constant parameters are set to the default values (Table S3 in ESM §3.2), except $T_{\max} = 10^8$.

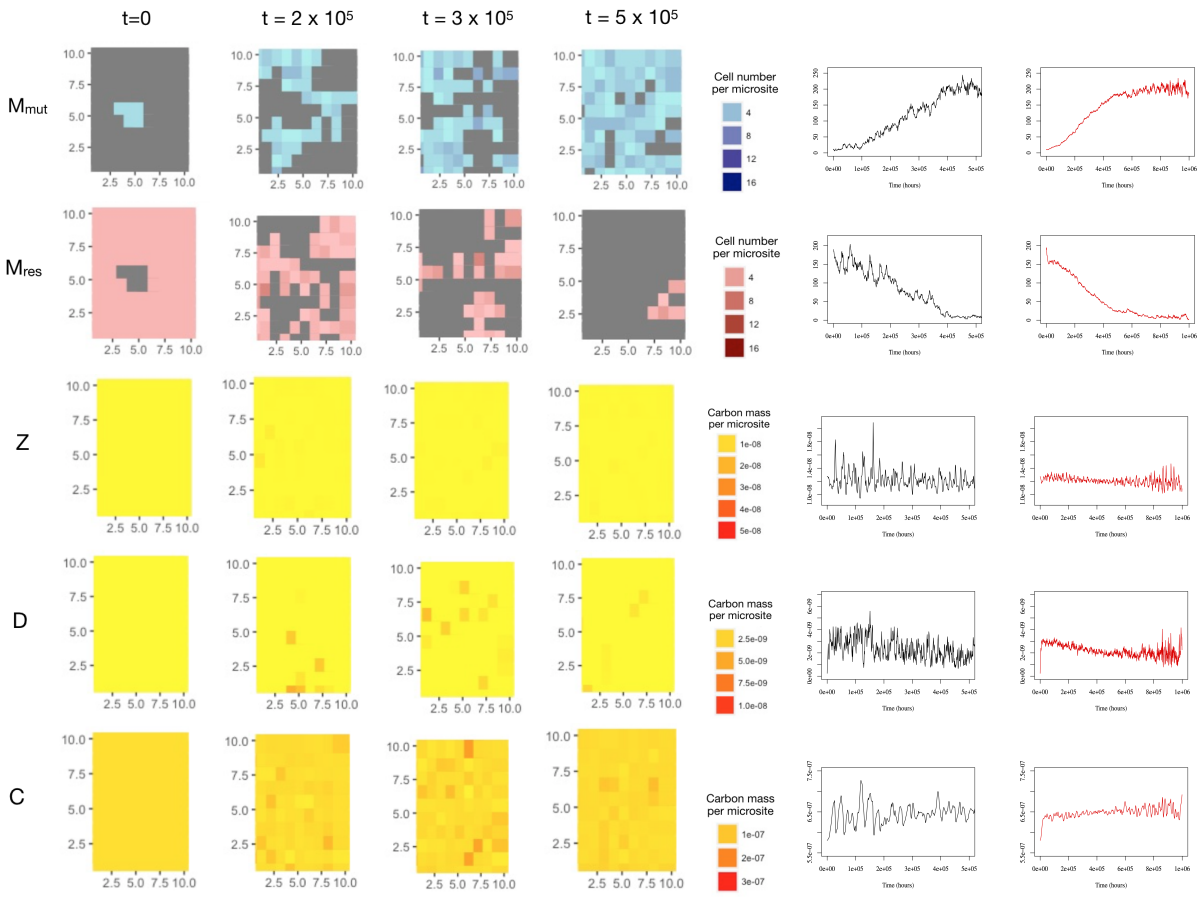

Figure 2. Spatio-temporal dynamics of invasion of a mutant cooperator ($\varphi_{mut} = 0.8$) into the ecosystem established by a resident strain investing slightly less in exoenzyme production ($\varphi_{res} = 0.75$). From top to bottom: temporal dynamics of the mutant cell population (M_{mut}), resident cell population (M_{res}), enzyme (Z), DOC (D), SOC (C). Columns 1-4: example simulation run of the spatial hybrid stochastic-deterministic model over a 10 x 10 lattice of microsites, snapshots from time $t = 0$ to $t = 5 \times 10^5$. Column 5: Aggregated dynamics of the simulation run across the lattice. Column 6: Mean trajectories, averaged over 20 replicated simulation runs. All constant parameters are set to the default values (Table S3 in ESM §3.2). The lattice was initialized with all microsites occupied by residents, except for five microsites occupied by mutants at the center of the lattice. All ecosystem variables z, c, d and M were fixed at the steady state determined by the established resident strain. See ESM §2 for simulation detail.

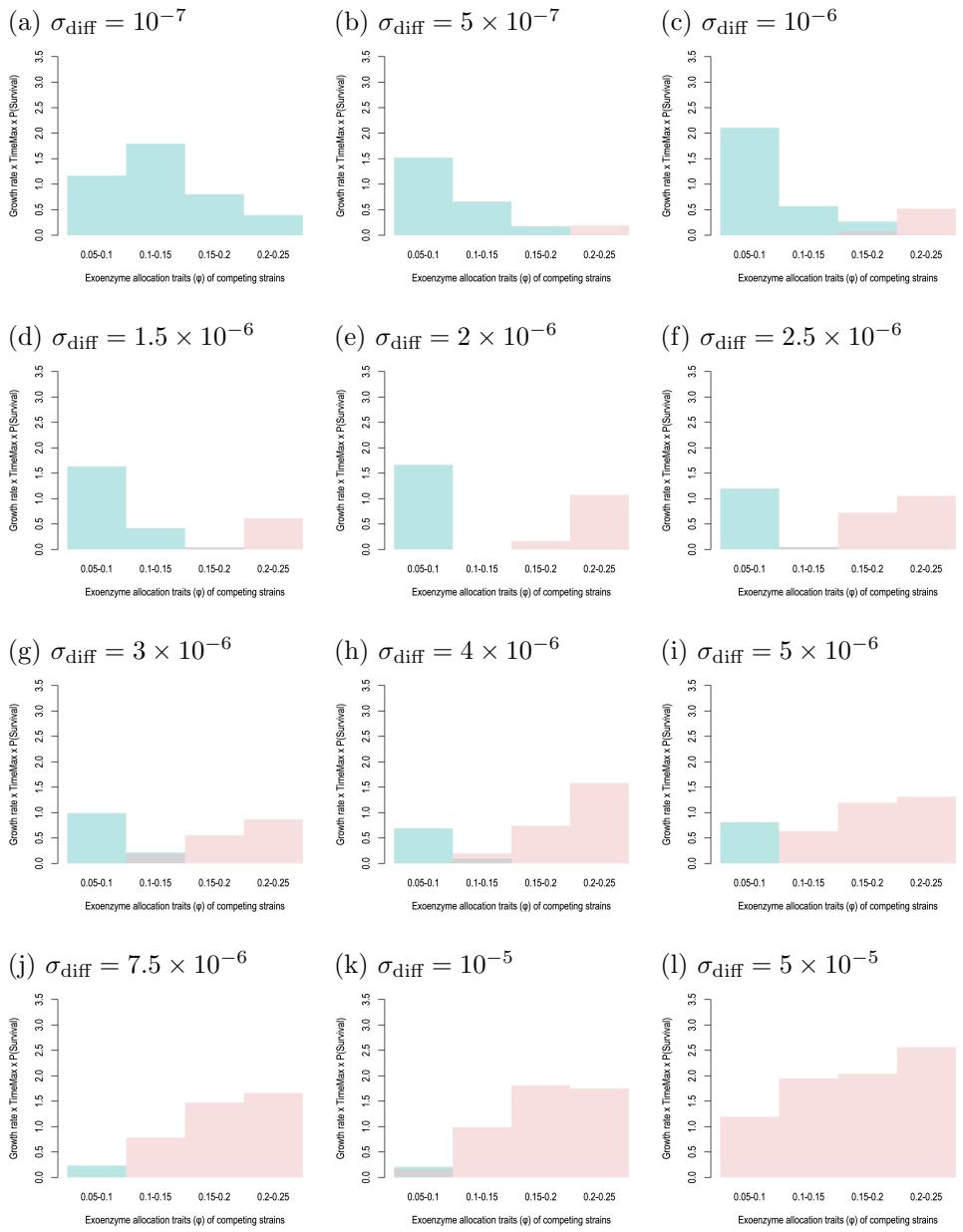

Figure 3. Patterns of selection on exoenzyme production at different soil diffusion rates. Each graph shows the mutant invasion fitness across pairwise resident-mutant competing strains. Invasion fitness is measured as the product of the mutant survival probability and the average long-term growth rate of growing mutant populations among stochastic simulation replicates. The survival probability is estimated as the fraction of simulations with a non-extinct mutant population at T_{max}. The long-term growth is calculated as the average of $(1/T_{max}) \log \frac{\text{final mutant population size}}{\text{initial mutant population size}}$ among all survival runs for each pairwise competition test, with $T_{max} = 10^6$. Red bars show invasion fitness of the cheater strain taken as mutant (with the lower φ value in the competing pair); blue bars show invasion fitness of the cooperator strain taken as mutant (with the higher φ value in the competing pair). Positive invasion fitness of cheater mutants (red bars) indicate selection against exoenzyme production. Positive invasion fitness of cooperator mutants (blue bars) indicate selection in favor of exoenzyme production. All constant parameters are set to the default values (Table S3 in ESM §3.2). Mutant initial population size is set to 5% of the abundance of the resident population in the central microsites. We tested values of σ_{diff} between 10^{-8} and 10^{-4} and report results for σ_{diff} between 10^{-7} and 5×10^{-5} as variation of σ_{diff} outside this range had no effect.

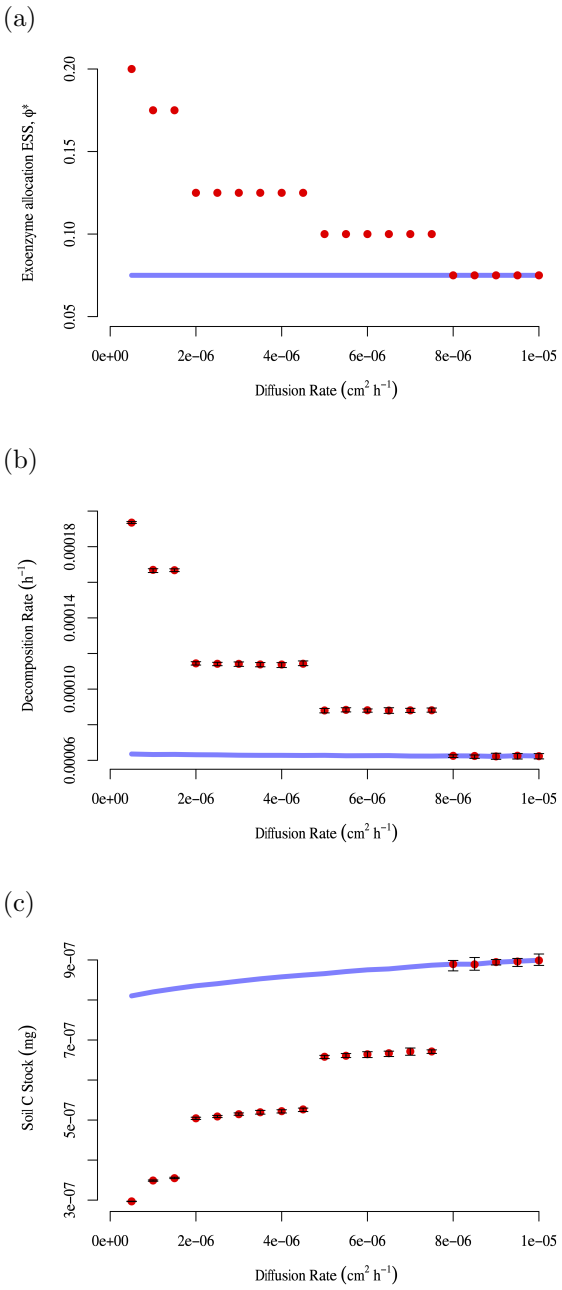

Figure 4. Effect of soil diffusion on the evolution of exoenzyme production and lattice-scale feedback on ecosystem function (decomposition rate and soil carbon stock), predicted by the spatial hybrid stochastic-deterministic model. (a) Red, Enxoenzyme allocation ESS as a function of diffusion. Blue, Exoenzyme allocation without evolutionary adaptation to variation in soil diffusion (fixed at ESS predicted for $\sigma_{\text{diff}} = 10^{-5}$). (b) Red, Feedback of exoenzyme allocation adaptation to lattice-scale decomposition. Blue, Lattice-scale decomposition as a function of diffusion, without microbial evolutionary adaptation. (c) Red, Feedback of exoenzyme allocation adaptation to lattice-scale carbon stock. Blue, Lattice-scale carbon stock as a function of diffusion, without microbial evolutionary adaptation. In (a), for each diffusion rate the ESS is approximated by the resident phenotype with minimum mutant invasion fitness extracted from Fig. 3. In (b) and (c), for each diffusion rate the exoenzyme allocation fraction is fixed at its corresponding ESS from (a). We then ran simulations of a monomorphic microbial population at ESS and calculated the decomposition rate (maximal decomposition rate times total enzyme mass) averaged across the lattice and the total SOC mass over the lattice, averaged over time (between time 2×10^5 and $T_{max} = 10^6$, to remove the initial transient). Error bars measure variation of the mean among simulations due to process stochasticity. All constant parameters are set to the default values (Table S3 in ESM §3.2). See ESM §2 for further simulation detail.

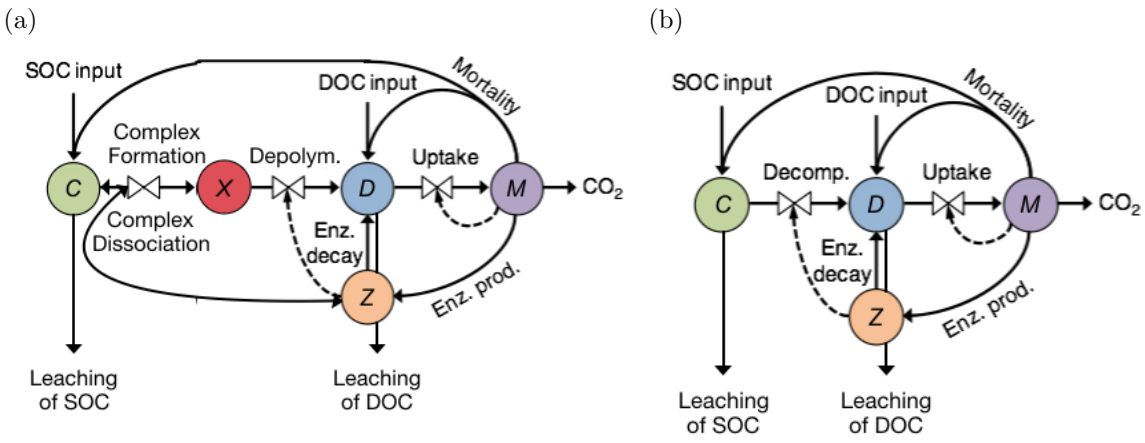

Figure 5. Microbe-enzyme driven decomposition of soil organic matter: Modelled entities and processes. (a), Five-compartment model. (b), Four-compartment model. SOC, soil organic carbon. DOC, dissolved organic carbon. Plain arrows indicate carbon fluxes among compartments and in and out of the system. Dotted arrows indicate the exoenzyme concentration dependence of the decomposition rate.